

Structures of the intracloud electric field supporting origin of long-lasting thunderstorm ground enhancements

A. Chilingarian,^{1,2,3} G. Hovsepyan,¹ S. Soghomonyan,¹ M. Zazyan,¹ and M. Zelenyy^{3,4}

¹*Alikhanyan National Lab (Yerevan Physics Institute), Yerevan 0036, Armenia*

²*National Research Nuclear University MEPhI, Moscow 115409, Russia*

³*Space Research Institute of RAS, Moscow 117997, Russia*

⁴*Institute of Nuclear Research of RAS, Moscow 117312, Russia*



(Received 15 August 2018; published 3 October 2018)

The problem of thundercloud electrification is one of the most difficult ones in atmospheric physics. The structure of electric fields in clouds escapes from the detailed *in situ* measurements; few balloon flights reveal these rather complicated structures. To gain insight into the problem of the charge structure of a thundercloud, we use new key evidence—the fluxes of particles from a thundercloud, the so-called thunderstorm ground enhancements—TGEs. TGEs originate from electron acceleration and multiplication processes in the strong electric fields in the thundercloud, and the intensity and energy spectra of electrons and gamma rays as observed on the Earth's surface are directly connected with the atmospheric electric field. Discovery of long-lasing TGEs poses new challenges for revealing structures in the thundercloud responsible for hours-extending gamma ray fluxes. In the presented paper, we demonstrate that experimentally measured intensities and energy spectra of the “thundercloud particles” give clues for understanding charge structures embedded in the atmosphere. A rather short “runaway” process above the detector site, which is consistent with the tripole structure of the cloud electrification, is changing to a much less energetic emission that lasts for hours. Measurements of enhanced particle fluxes are accompanied by the simulation experiments with CORSIKA and GEANT4 codes.

DOI: 10.1103/PhysRevD.98.082001

I. INTRODUCTION

One of the main problems of the atmospheric electricity is the study of the spatial-temporal structure of the electric field in the thunderclouds. Precise measurement of the electric potential within thunderclouds is extremely difficult because of the time variability and the need to make spatially separated simultaneous measurements within the highest field regions of the storm [1]. The charge structure of a thundercloud can be viewed as a vertical tripole consisting of three charge regions. The main positive charge region is located at the top, the main negative in the middle, and an additional positive below the main negative [2]. Reference [3] observed a tripole charge structure, with a large lower positively charged region (LPCR) in the thunderclouds over the Tibetan plateau of China, and noticed that the large LPCR prevents negative cloud-to-ground (CG) flashes from occurring and, instead, facilitates inverted-polarity intracloud (IC) flashes. Different lightning scenarios that may arise depending upon the magnitude of the LPCR have been examined in [4]. Reference [5] examined different patterns of the near-surface electric field occurring during the thunderstorm ground enhancements (TGEs, [6,7]). A hypothesis that electrons of the ambient population of cosmic rays are accelerated and multiplied in the bottom dipole formed by

the main negative charge layer and the LPCR was proposed. Reference [8] also considered the electric field of the same direction formed by the main negative charge in the cloud and its mirror image on the ground.

The possibility that the intracloud electric field could be evaluated by ground-based measurements of the gamma ray and electron spectra was considered in [9]. However, there were only a few cases when electron energy spectra were measured at the ground level [10] due to fast attenuation of the electron flux in the air. Nonetheless, measured gamma ray spectra are in good agreement with the RREA model [11,12].

The relation of particle fluxes and lightning flashes also provides valuable information on the cloud electrification. During the TGE, lightning flashes are suppressed, and, when this happens, they usually abruptly terminate the high-energy particle flux [13,14]. Simultaneous detection of the particle fluxes and atmospheric discharges with microsecond time resolution on Aragats enables us to associate the lightning types abruptly terminated particle fluxes with the electric structure within thundercloud [8].

However, the TGE-electric field relation is still far from fully understood, and the study of various charge structures that can initiate the TGEs should be accompanied by Monte Carlo simulation of the passage of particles through the region of the assumed intracloud electric fields.

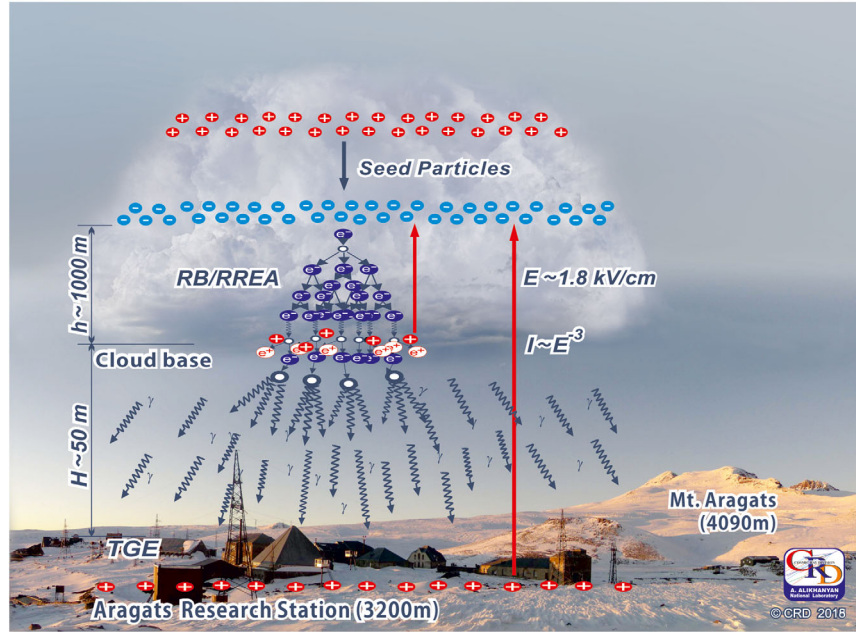


FIG. 1. Cartoon demonstrating electron acceleration and multiplication in the electric field of the lower dipole of the thundercloud and in the electric field beneath the cloud.

Thus, we use a new type of key evidence in the atmospheric electricity research, namely, the particle fluxes from the thunderclouds, to scrutinize the atmospheric electricity problem. The origin of the fluxes of electrons, gamma rays, and neutrons detected on the Earth's surface are the runaway breakdown (RB) processes [15] now mostly referred to as relativistic runaway electron avalanches (RREA, [16,17]). The electron acceleration in the Earth's direction is due to the electric field between the main negative charge region in the middle of the cloud and the positive charge that is induced on the ground. This field can be significantly increased by the electric field between the main negative region and the emerged lower positively charged region (LPCR) in the bottom of the cloud. The maximal intensity (and maximal energy of particles) of the TGE is observed when the strength of the total electric field in the cloud exceeds the “runaway” threshold in the atmosphere and the RB/RREA avalanches start to develop in the direction of Earth. Such a condition corresponds to the maximum dimension and charge of the LPCR; thus, the lightning leader cannot make its path through the LPCR, and cloud-to-ground flashes are suppressed [4]. The decay of the gamma ray flux and its termination by the lightning flash indicates the degradation of the bottom dipole.

In the presence of weak electric fields in the atmosphere (lower than RB/RREA threshold) when cosmic ray seed electrons cannot “runaway” and originate avalanches, the electric field effectively transfers energy to the electrons modifying their energy spectra (MOS process, [18]) and making the probability of emitting bremsstrahlung gamma rays larger. In contrast to RB/RREA, the MOS process is

dominating in the energy range above ≈ 50 MeV; the RREA process generates gamma rays with energies below ≈ 50 MeV although with a much larger count rate.

In the cartoon (Fig. 1), we show the electron–gamma ray avalanche developed in the bottom of the thundercloud above the Aragats high altitude research station of the Yerevan Physics Institute [19]. The avalanche comes out of the base of the cloud and illuminates various particle detectors, measuring count rates of charged and neutral particles and their energy. The distance to the cloud base at Aragats in the spring and autumn seasons is usually rather small $H = 25\text{--}100$ m; in summer, it is larger, $H = 50\text{--}500$ m. In our simulation studies of TGEs, we will assume the strength of the electric field in the cloud up to 1.8 kV/m and elongation up to 1 km. Both values are ordinary and have been measured in balloon flights [20].

The recently discovered phenomenon of long-lasting TGEs [21] gives additional clues to understanding embedded charged structures in thunderclouds. With numerous observations of TGEs in the 2017–2018 seasons and incorporated appropriate Monte Carlo simulations, we will demonstrate how intracloud electric fields originate the particle fluxes that continue for hours.

II. DISTURBANCES OF THE NEAR-SURFACE ELECTRIC FIELD DURING TGES

The spring season on Aragats usually continues from April to middle of May. It is characterized by low-lying clouds (25–100 m); high relative humidity (RH) of 95%–98%; large disturbances of the near-surface electric field

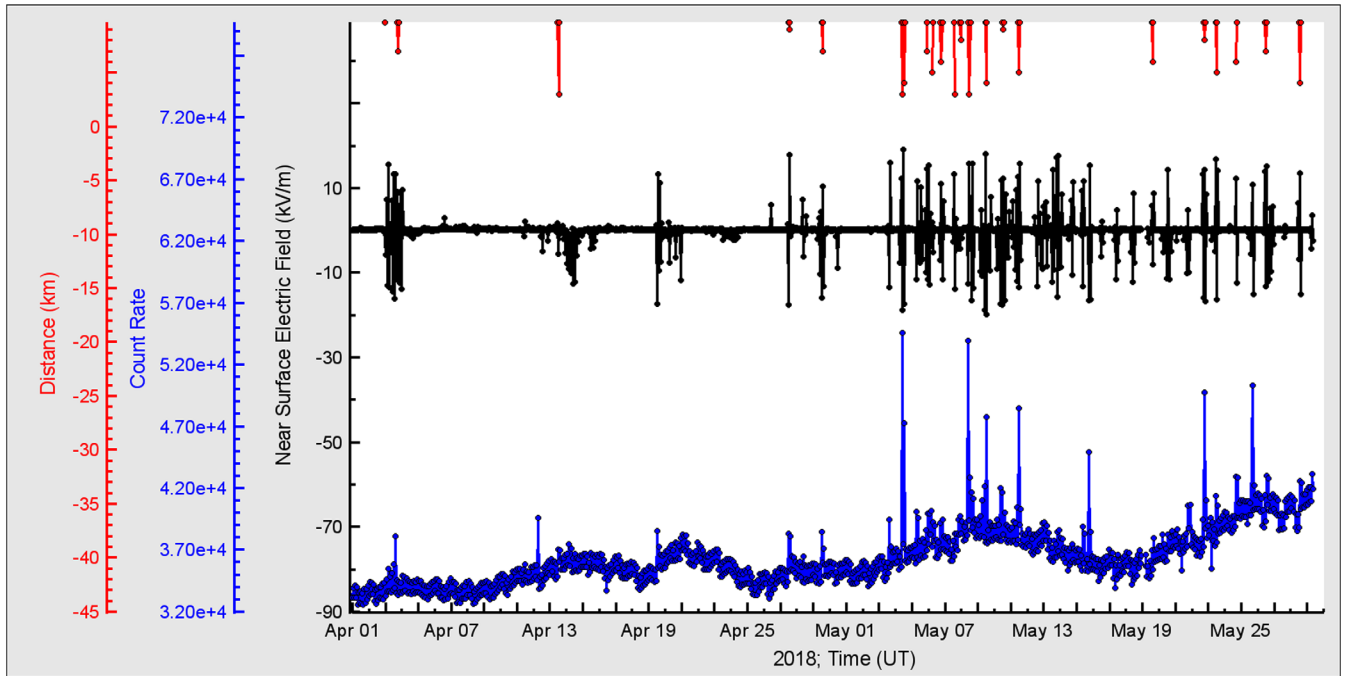


FIG. 2. At the top, vertical lines show the distance to lightning flash; in the middle, we show near-surface electric field disturbances measured by EFM-100 electric mill; at the bottom, one-minute time series of 1-cm-thick 1 m²-area outdoor plastic scintillator located outdoor nearby MAKET experimental hall.

(sometimes dropping into the negative region down to -30 kV/m for several minutes); intense lightning activity (approaching the station for a few kilometers), and numerous TGEs—see Fig. 2. Large TGEs occurred usually when the outside temperature was in the range from -2 to $+2$ C° degrees.

In Fig. 2, we see that TGE activity peaked in the first days of May, providing multiple episodes of large fluxes of electrons and gamma rays. The mean count rate of the outdoor scintillator is increasing in May due to melting of the snow covering it in winter months (mean count rate is also dependent on the atmospheric pressure).

On May 22, 2018, thunderclouds approached the borders of Armenia, moving as usual from the Armenian highlands into Turkey. In Fig. 3, we show the approaching front of the storm as mapped by atmospheric discharges registered by the Boltek StormTracker lightning detector. At 16:00, the electrified clouds reached the Aragats mountain environment, inducing large disturbances of the near-surface electric field accompanied with lightning flashes; see Fig. 4.

In Fig. 4, we show the typical spring TGE with several maxima of high-energy particle (HEP) emissions, coinciding, as a rule, with the episodes when the near-surface electric field dropped into the deep negative region for at least several minutes. The emerging structures in the measured time series of the near-surface electrostatic field posted in the middle of Fig. 4 are reflecting the complicated structure of charged layers in the thundercloud. We speculate that when the mature LPCR arrives (or emerges) above

the detector location, the strength of the electric field in the lower dipole reaches the “runaway” threshold, and an unleashed electron-photon avalanche provides the maximum flux of TGEs. The intensity of the particle flux reaches the maximum if the LPCR is above the detector; when the cloud moves away from the detector site, the TGE declines.

In Fig. 4, along with the disturbances of the electric field, we also show the time-series of count rates of large NaI crystals. After the peak, the prolonged tail of the TGE is comprised of the low-energy gamma rays (with max energy 3 MeV or less). The NaI spectrometers have energy threshold of ≈ 0.3 MeV, besides the fifth one, whose threshold is ≈ 3 MeV. Thus, spectrometers with a higher-energy threshold register only peaks of TGE; they do not detect the long-lasting “pedestal” which comprises the low-energy particles.

At 20:15–22:15, without noticeable disturbances of the near-surface electric field, the NaI crystals continue to register decaying gamma ray flux. To gain insight into these two modes of the cloud radiation, we look at the electric field disturbances in more detail.

In Fig. 5, we show a zoomed version of the near surface electric field along with the count rate of the 1-cm-thick outdoor plastic scintillator (rather good coinciding with count rate of the NaI network), outside temperature, dew point, and relative humidity. From the picture, it is apparent that the most important feature, which is responsible for the particle burst, is the sufficiently long time period during which the near surface electric field remains

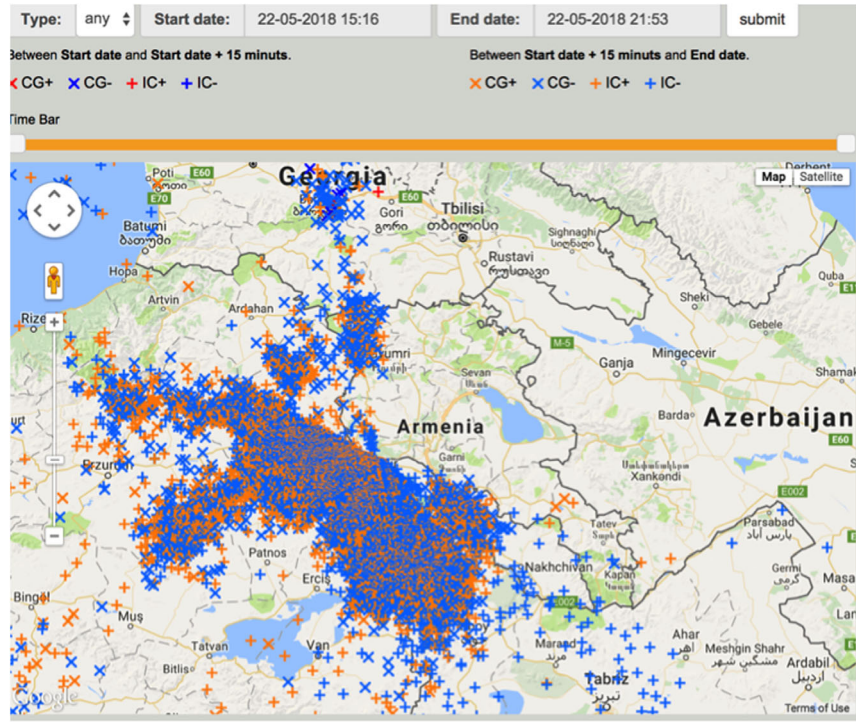


FIG. 3. The Google Map with lightning flashes shows the thunderstorm of May 22, 2018, approaching Armenia.

in the deep negative domain (≈ -15 kV/m). We measure the peak significance in the units of relative enhancement (percent) and in numbers of standard deviations from the mean value measured before the TGE started (critical

value of the peak significance test, $N\sigma$). The critical value (and corresponding p-value—integral of probability density distribution from the critical value to infinity) is the most comprehensive estimate of the reliability of detecting

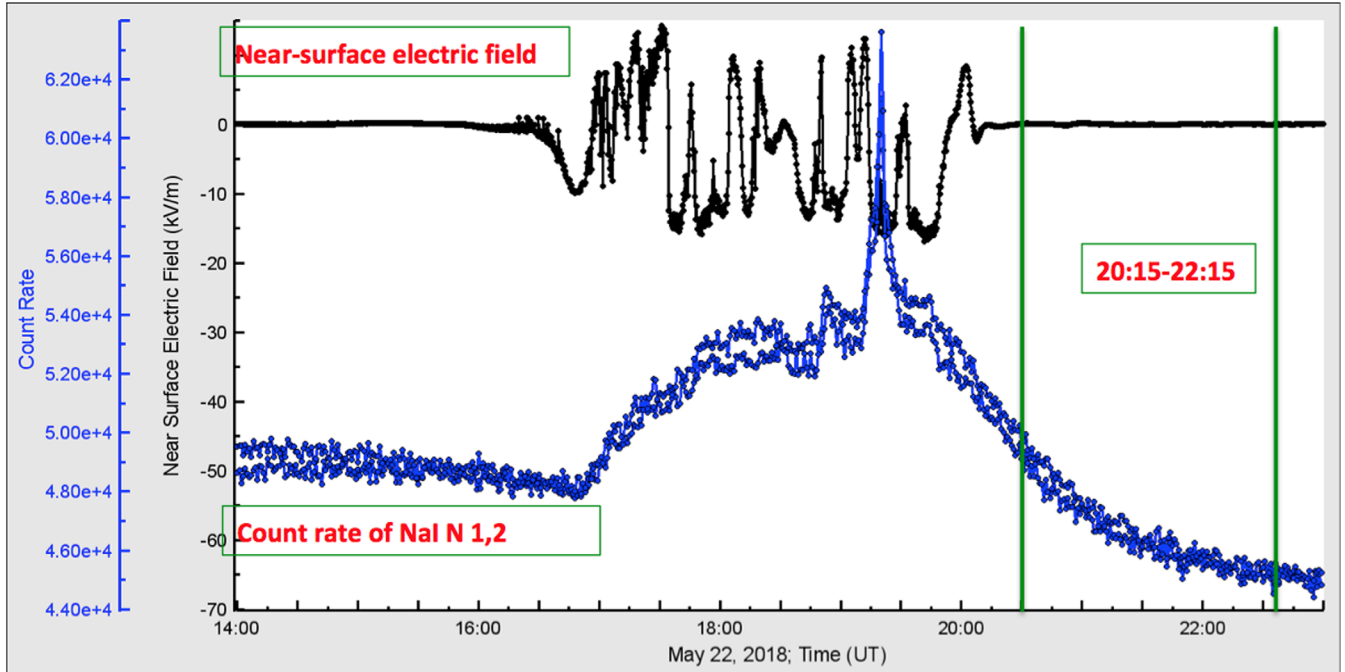


FIG. 4. LL TGE lasting approximately from 17:00 to 22:15; at the top, disturbances of the near-surface electric field measured by the EFM-100 electric mill located on the roof of MAKET experimental hall; at the bottom, one-minute time series of the NaI network's spectrometers N 1 and 2 (energy threshold 0.3 MeV). The inset shows time series of NaI N5 spectrometer (energy threshold 3 MeV).

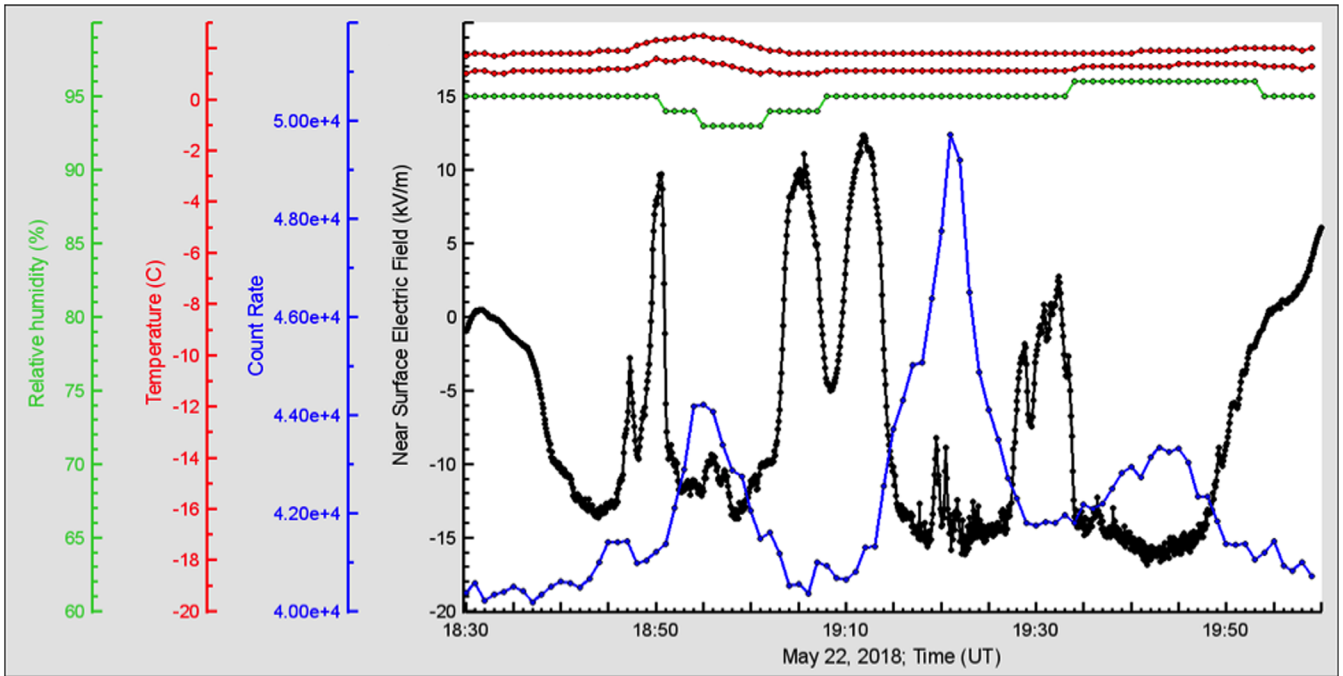


FIG. 5. Triple peak structure of HEP TGE: in the top outside temperature, dew point, and relative humidity.

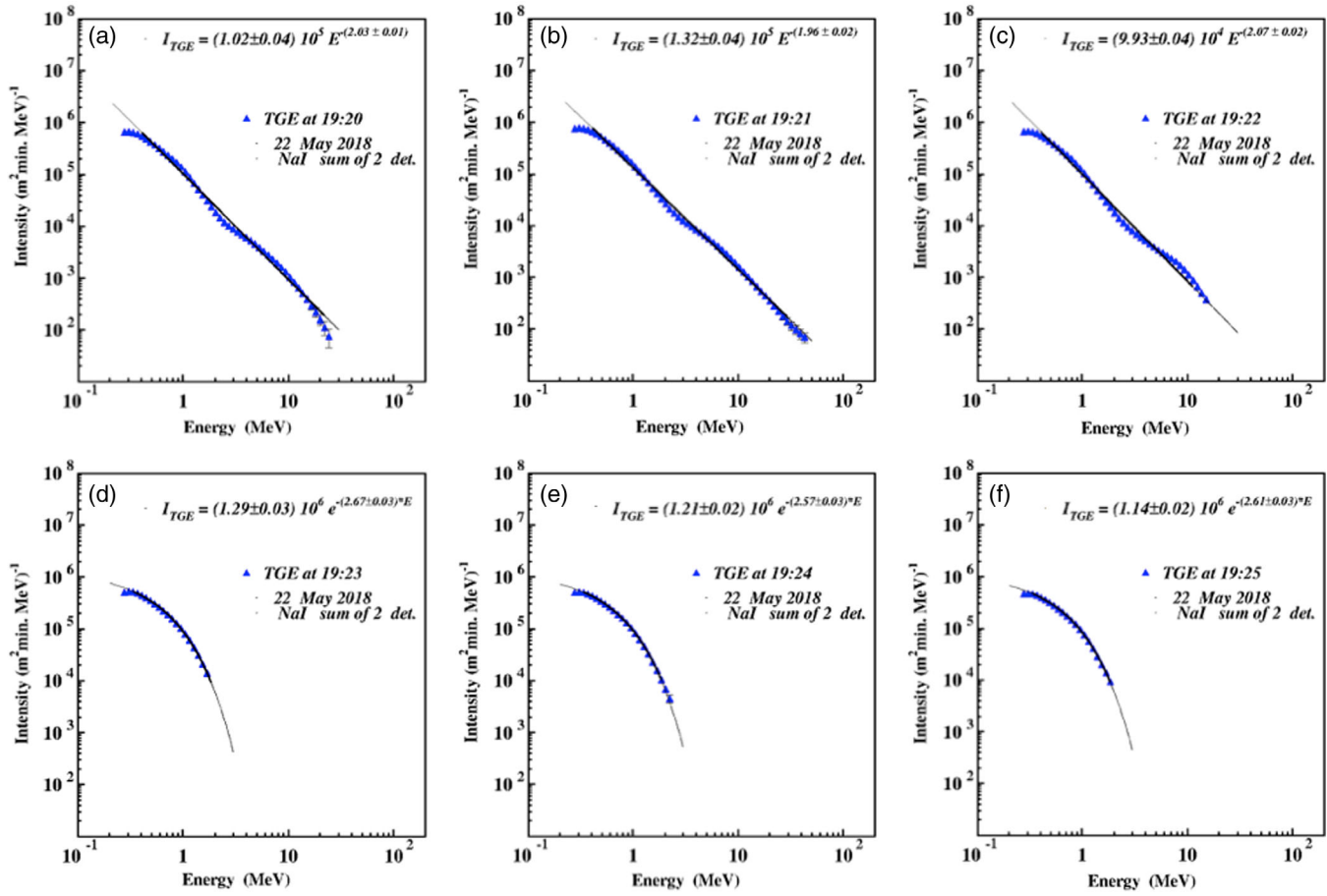


FIG. 6. The differential energy spectra of TGE particles registered by NaI network (N 1 and N 2 spectrometers); minutes 19:20–19:26.

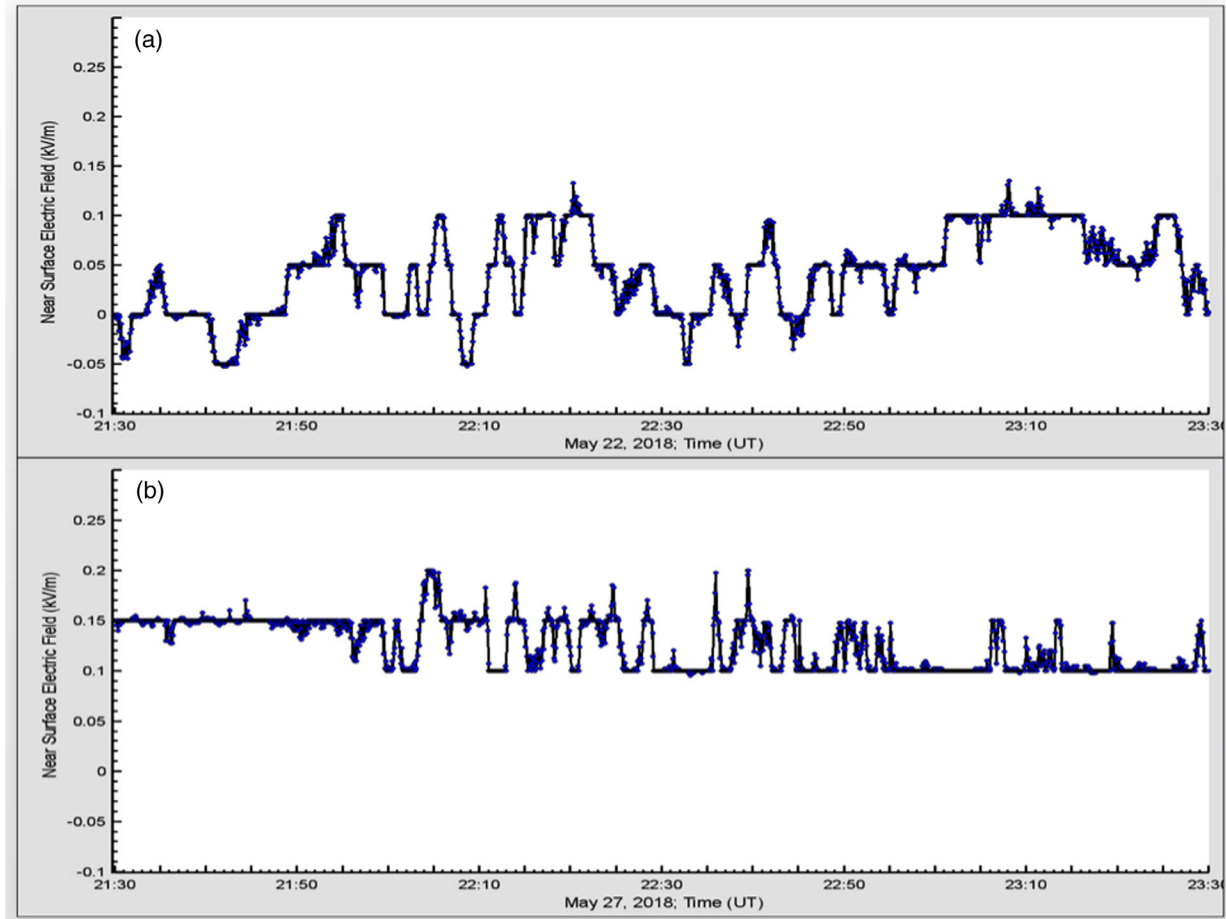


FIG. 7. The disturbances of near-surface electric field measured by EFM-100 electric mills with a sampling rate of 1 Hz on Aragats during LL TGE (6a), and during fair weather (6b).

peaks in the time-series. Large critical values correspond to small probabilities that the observed peak is a background fluctuation and not a genuine peak (TGE). Therefore, we can safely reject the null hypothesis (background fluctuation) and confirm the TGE. Very large critical values not only prove the unambiguous existence of a particle flux from the cloud but also serve as a comparative measure of the TGE observations using different detectors. During first peak (significance $\approx 13\% / 13\sigma$), near-surface field values were below -10 kV/m at 18:52–19:01, 9 min; during middle largest peak (significance $\approx 30\% / 30\sigma$) at 19:15–19:28, 13 min; for the third peak (significance $\approx 12\% / 12\sigma$) at 19:34–19:49, 15 min. These extended periods of negative field were accompanied by small outbursts with field strength of several kV/m . We speculate that these outbursts are possibly connected with the LPCR emergence. However, outbursts are small and, therefore, the LPCR is not mature. The location of the cloud base estimated by the, so-called, “spread” parameter [22] is $\approx 100 \text{ m}$; the relative humidity is $\approx 95\%$; the maximal count rate measured by the 1-cm-thick and 1 m^2 area outdoor plastic scintillator reaches 50,000 per minute.

For understanding the relation between HEP bursts and long-lasting, low-energy emissions, we measure differential energy spectra during full duration of the TGE. In Fig. 6, we show the energy spectra of the LL TGE. To obtain a pure TGE signal, the cosmic ray background (containing muons, neutrons, and other energetic particles) measured at fair weather just before TGE should be bin-by-bin extracted from the histogram containing both background and additional counts from the avalanches initiated in the thundercloud. After background extraction, the histogram is fitted by an analytical distribution function (usually power law or exponential). For the recovery of the differential energy spectra measured by the NaI network, the spectrometer response function was calculated with the CERN GEANT package.

The sizeable intensity TGE was observed during 3 minutes (19:20–19:22). At the beginning [Fig. 6(a)] and in the end [Fig. 6(c)] of the high-energy TGE, the maximal energy of the flux reached 20 MeV and, at the minute of maximal flux [Fig. 6(b)], -40 MeV . The particle flux was well approximated by the power law dependence with spectral index ≈ -2 . After fading of the high-energy particle, the shape of the flux spectrum abruptly changed to

exponential dependence with maximal energy not exceeding 3 MeV. Such an abrupt change of the flux shape spectrum and maximal energy can be connected with transient structure in the intracloud electric field. We associate it with the lower positively charged region, which significantly enhanced the total flux in the cloud for a few minutes. The charge and size of the main negatively charged region in the middle of the cloud is at least an order of magnitude larger than the charge and size of the LPCR. Thus, for a few minutes when the LCPR develops, the field in the cloud exceeds the runaway threshold, and the electrons which enter this enhanced field region are accelerated and multiplied, producing the TGE on Earth's surface. As the cloud is rather high (≈ 100 m), due to the attenuation of particle flux in the air, the significance of the TGE does not exceed $\approx 30\%$ corresponding to ≈ 30 standard deviations.

As we can see in Figs. 4 and 6, the gamma ray flux is lasting for hours after the disturbance of the near-surface electric field calms down. To check the exact pattern of electric field fluctuations, we compare the electric field measured by electric mill EFM-100 just after TGE and at the same time during a fair weather period. In Fig. 7(a), we can see that the disturbances measured by the electric mill during TGE are not very large, but not negligible, and have excursions to the negative domain. For the fair weather, the field value never goes below 0.1 kV/m, and variance is much smaller [Fig. 7(b)]. For the post-TGE electric field, the near-surface electric field values differ from the expected value of ~ 140 V/m typical for the fair weather [Fig. 7(b)]. The electric field strength difference of the fair weather and post-TGE electric field is 0.9 kV/m. In the next section, we will analyze small disturbances of the near-surface electric field, which accompany the small TGE events.

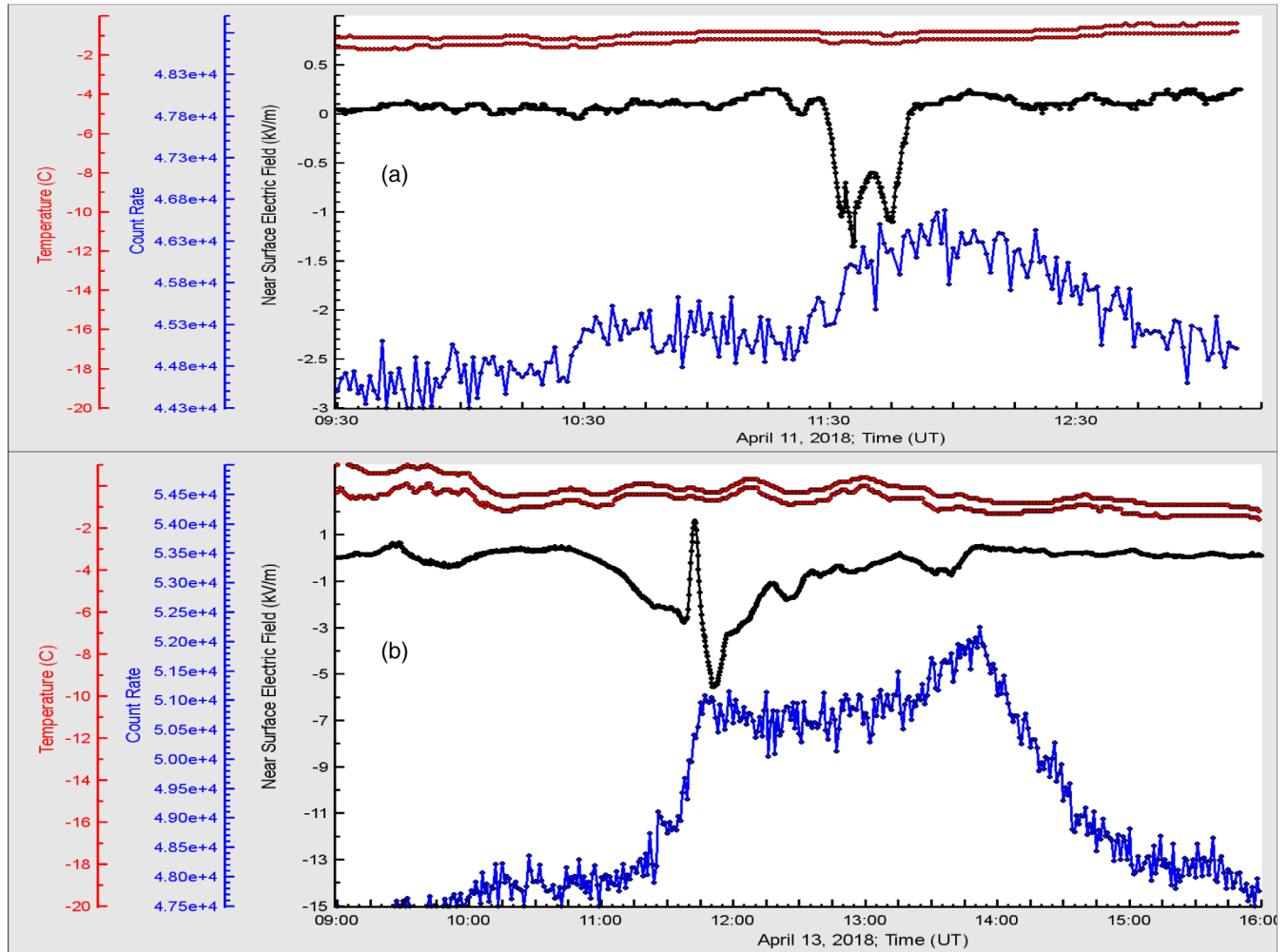


FIG. 8. Small TGEs observed in April 2018. At the top of each frame, we show outside temperature and dew point; in the middle, disturbances of the near-surface electric field; at the bottom, one-min count rate measured by the NaI crystal (energy threshold—0.3 MeV).

III. LOW-ENERGY LONG-LASTING GAMMA RAY FLUXES FROM THUNDERCLOUDS

In the previous section, we outlined some specific characteristics of the field disturbance pattern that are supporting TGEs. The TGE observed in the low-energy particle flux is very different from the one observed in the high-energy flux. The high-energy particles (HEP) come from RB/RRE avalanches unleashed above the detector site; particles are accelerated in the lower dipole of the cloud formed by the main negative layer and emerged LPCR. As we have seen in the previous section, the necessary conditions for the high-energy particle bursts are the deeply negative near-surface electric field and the closeness of the cloud base to the Earth's surface. During the high-energy phase of TGEs, the amplitude of disturbances of the near-surface electric field can reach 60–70 kV/m. However, we observe also the TGE events not connected with large disturbances of the electric field and lightning activity. Both the amplitude of disturbances and the significance of peaks are much smaller compared

with TGEs containing HEP. In Fig. 8, we show two such events that occurred in April 2018.

Estimated parameters for the April 11 event [Fig. 8(a)] are the following:

- (i) Duration of TGE: 11:25–12:45, 80 min;
- (ii) Duration of field disturbances 11:32–11:46, 13 min;
- (iii) Estimate of the height of cloud base: $(-0.8\text{--}1.2)\text{ C}^\circ * 122 \text{ m} \approx 50 \text{ m}$
- (iv) Relative humidity (RH) $\sim 97\%$;
- (v) TGE significance (NaI crystal) -4.8% (10.4σ).

TGE observed two days later was more prolonged and larger:

- (i) Estimated parameters for April 13 event [Fig. 8(a)] are as following:
- (ii) Duration of TGE: 11:25–12:45, 80 min;
- (iii) Duration of field disturbances 11:32–11:46, 13 min;
- (iv) Estimate of the height of cloud base: $(-0.8\text{--}1.2)\text{ C}^\circ * 122 \text{ m} \approx 50 \text{ m}$
- (v) Relative humidity (RH) $\sim 97\%$;
- (vi) TGE significance (NaI crystal) -4.8% (10.4σ).

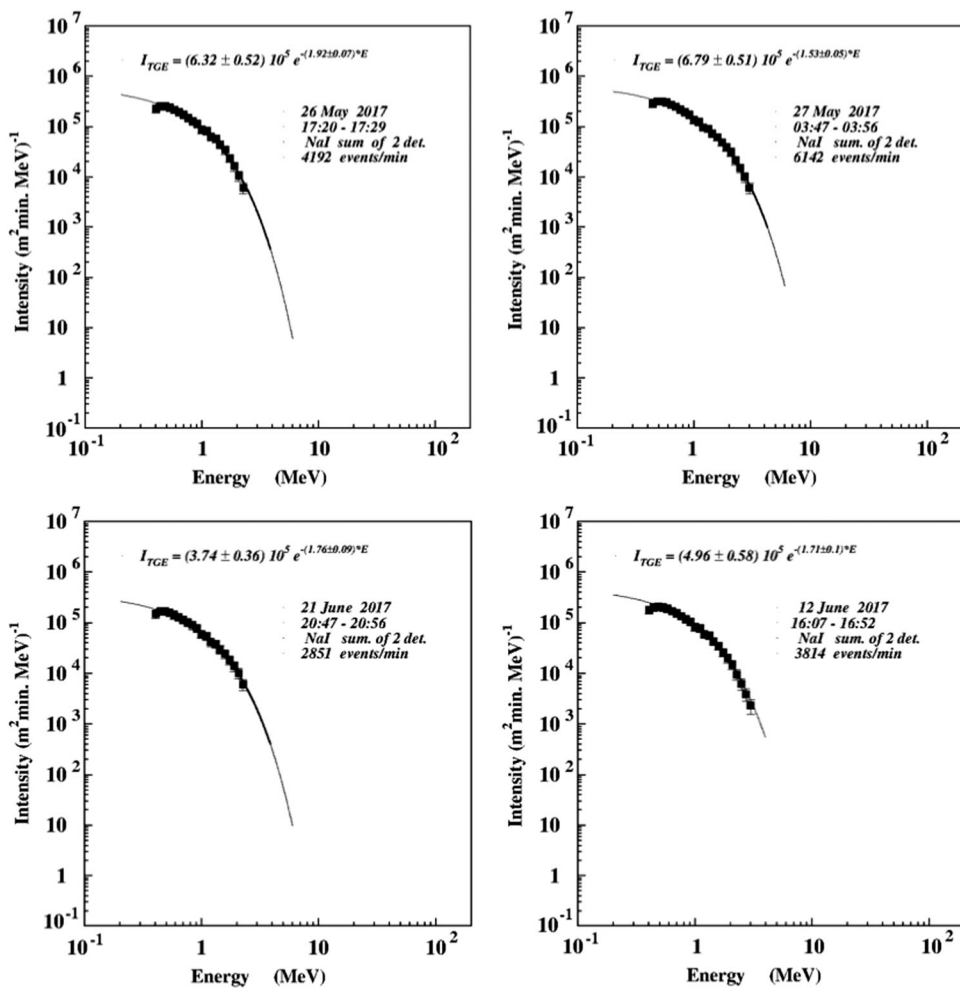


FIG. 9. Energy spectra of the TGE events coinciding with small disturbances of the near-surface electric field (possibly pure MOS process).

Neither TGE observed in April 2018 contained HEP or was accompanied by lightning activity.

Thus, there are two independent processes related to the particle fluxes from the thundercloud: the intense burst of particles from RB/RRE avalanches connected with LPCR development and prolonged low-energy gamma ray flux due to a MOS process [11]. The first one operates between the main negative charged layer and the LPCR; the second operates between the same main negative charged layer and the positive charge in the ground induced by the main negative charge. Thus, radiation processes in the clouds are not only connected with avalanches unleashing in the presence of the electric field above a threshold. Weak electric fields well below the RB/RREA initiation threshold also enhance gamma ray fluxes, although much less intensely than those with RB/RREA. Such small events can be fitted by a simple exponential dependence, with index varying from 1.5 to 1.9; see Fig. 9.

IV. TGES AND LIGHTNING FLASHES

In Fig. 10, we show the TGE observed by the one-cm-thick, one-m² area outdoor plastic scintillator on May 6, 2017. At 12:35, the electric field fell into the deep negative domain and remained there for \sim 12 minutes. Thus, a lower dipole was formed and started to accelerate electrons downwards in the direction of the Earth. On the Earth's surface, all particle detectors register sizable TGE (the peak p-value for 1-minute count rate detected by 1 m² area plastic scintillator was \sim 50 σ). Two lightning flashes

terminated the particle flux at 12:42:22 count rate drops from 665 to 547 in two s and at 12:47:38 from 664 to 490 in 4 s. Both flashes were identified as a negative cloud-to-ground (CG) (see Fig. 12 and explanation in the text below). Thus, negative CG lightning partially destroyed the lower dipole; however, it was recovered in a few seconds, and the TGE was reestablished two times in five minutes.

In Fig. 11, we show the differential energy spectra as one-minute histograms slices. The arrows denote lightning flashes. Each time after lightning, the high-energy portion of the TGE is declined. Thus, the lightning flash decreases the strength of the electric field in the lower dipole and electrons cannot "run away" anymore and accelerate to tens of MeV. However, the electric field in the cloud is still sizable to enhance gamma ray radiation by the MOS process.

Electromagnetic emission produced by two mentioned lightning flashes was detected by a fast wideband (50 Hz to 12 MHz) electric field measurement system. We used a 52-cm-diameter circular flat-plate antenna followed by a passive integrator (decay time constant = 3 ms), the output of which was connected via a 60-cm double-shielded coaxial cable to a Picoscope 5244B digitizing oscilloscope. The sample interval of the oscilloscope was 40 ns, and the recorded length was 1 s. The oscilloscope was triggered by the signal from a commercial MFJ-1022 active whip antenna that covers a frequency range of 300 kHz to 200 MHz.

The fast electric field record of the first flash that occurred at 12:42:23.501 shows characteristic return stroke (RS) signatures, which are indicative of-CGs (Fig. 12).

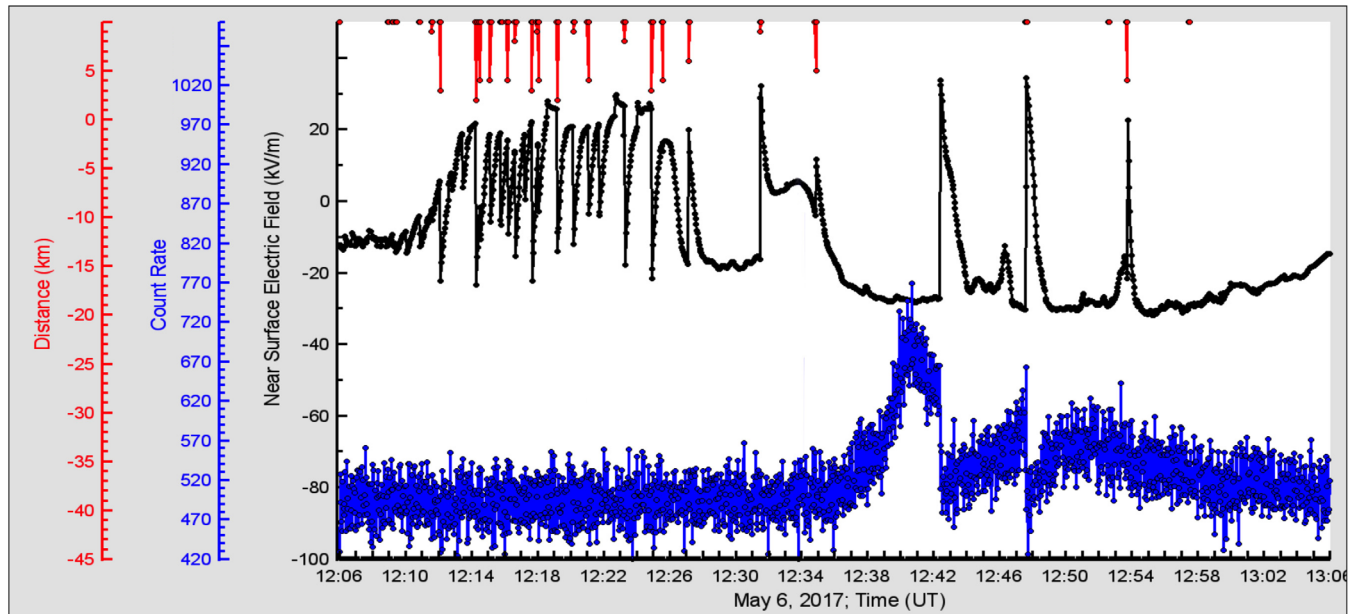


FIG. 10. From top to bottom: distance to lightning flash; disturbances of near surface electric field; one-second time series measured by 1-cm-thick outdoor plastic scintillator (energy threshold 0.7 MeV).

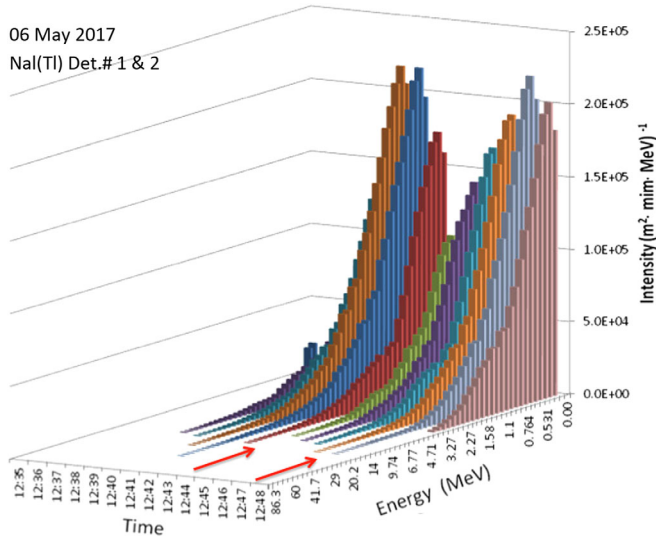


FIG. 11. The differential energy spectra measured by the NaI crystals minute-by-minute during TGE. By red arrows are denoted lightning flashes terminated high-energy particle flux.

Two RS pulses are observed at 177.6 ms and 210.8 ms after the trigger. The fast electric field record of the second flash that occurred at 12:47:36.302 also shows characteristic return stroke (RS) signatures, which are indicative of CGs. Four RS pulses are observed at 462.7 ms, 474.2 ms, 587.1 ms, and 787.6 ms after trigger; see Fig. 12.

V. MONTE CARLO SIMULATION OF PARTICLE PROPAGATION IN THE INTRACLOUD ELECTRIC FIELD

In previous sections, we show that TGEs can last for many hours and comprise short high-energy bursts and extended lower-energy gamma ray flux. To check these findings, we performed simulations with CORSIKA and GEANT4 codes [23,24]. The theoretical bases of our simulation experiments are well-known processes of charged and neutral particle interactions with the terrestrial atmosphere and very simple models of cloud electrification. We assume the presence of the positive electric field of

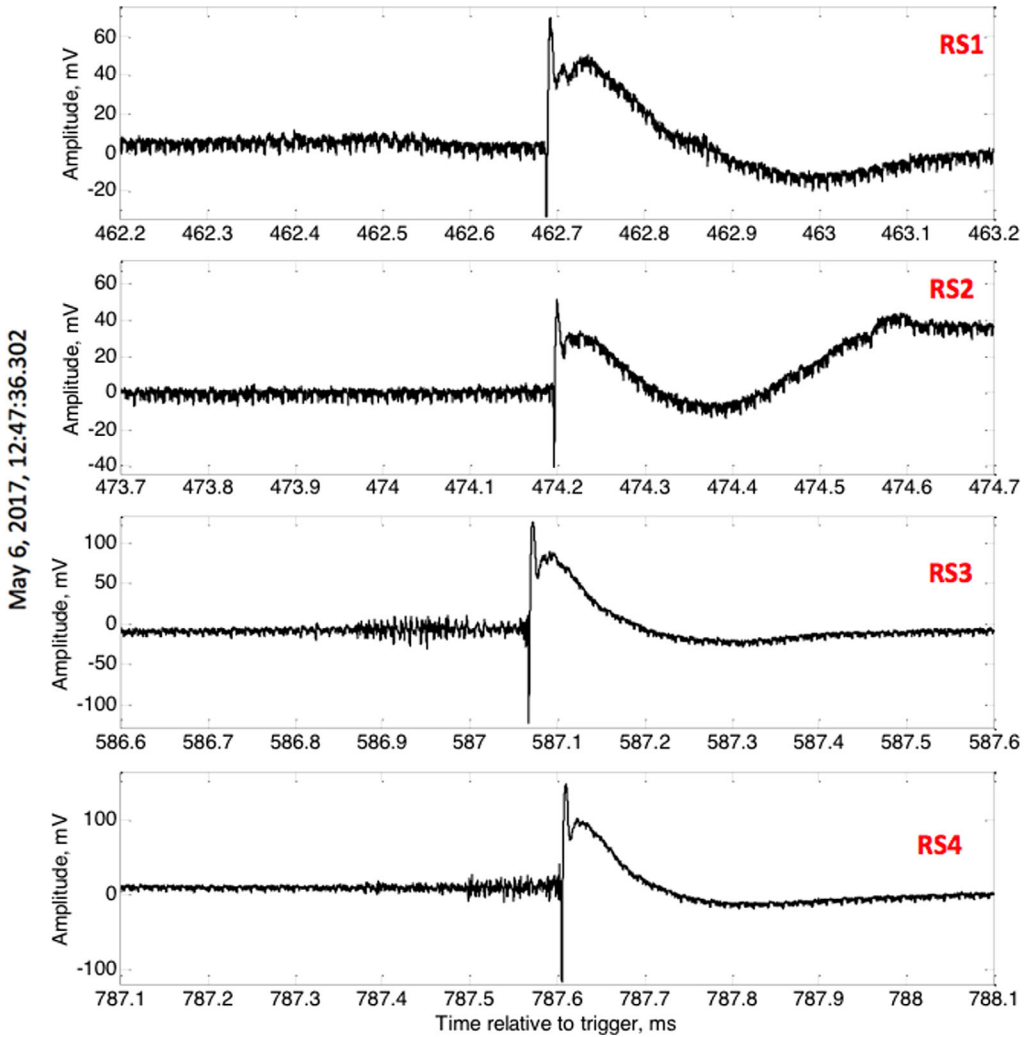


FIG. 12. Four RS pulses are observed at 462.7 ms, 474.2 ms, 587.1 ms, and 787.6 ms after trigger at 12:47:36/302.

different strength and spatial extent in the lower part of the cloud; the cloud base height was selected according to measurements on Aragats. Each simulation trial consists of 10^8 vertical gamma ray and electron showers with energies in the interval 1–100 MeV. The differential energy spectrum of gamma rays from the ambient population of cosmic rays follows the power law with spectral index $\gamma = -1.42$ (on the heights 4–5 km). We follow the cascade particles till their energy is above the energy cutoff of $E = 0.05$ MeV. The observation level $H_{\text{obs}} = 3200$ m above sea level is the Aragats research station elevation. In Fig. 13, we show the dependence of enhanced particle flux on the strength of the electric field in the cloud changing from 0.1 to 1, 8 kV/cm. The spatial extent of the electric field was 1 km, and the height of the cloud base above the detectors was 50 m; see Fig. 1 for the arrangement of simulations.

In Fig. 13, we can see that although particle flux is dramatically enhanced by reaching the RB/RREA threshold (≈ 1.8 kV/m on 4000 m height above sea level), the enhanced particle fluxes are nonetheless also evident for smaller electric fields. We assume that these electric fields originate in the cloud below the main negatively charged layer and extend to Earth's surface. Starting from the lowest tested field of 0.1 kV/m, we can see small enhancements of particle flux in good agreement with observations. Thus, the low electric fields in the atmosphere above the detector site can explain prolonged gamma radiation after the high-energy phase of TGE.

Another possible explanation of the long-lasting gamma ray flux is the detection of Compton-scattered gamma rays from the remote RB/RRE avalanches. According to our views, the RB/RRE avalanches are continuously emerging in the different parts of the thundercloud filling it with radiation [25]. To test the possibility of detecting remote RRE avalanches, we investigate the radial distribution of the gamma ray flux originated from large TGE. Each simulation set consists of 10^8 vertical gamma ray showers initiated by particles with energies in the interval 1–100 MeV (the differential energy spectrum was a power law, spectral index $\gamma = -3$), leaving the cloud on different heights

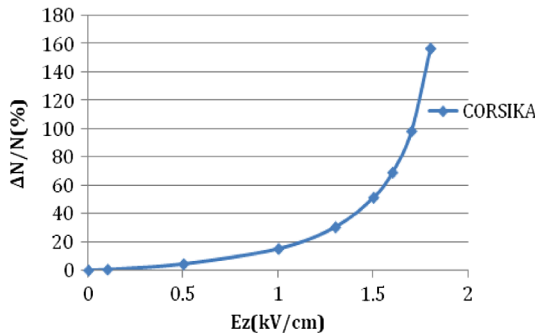


FIG. 13. Dependence of particle flux on the strength of the 1 km extended intracloud electric field.

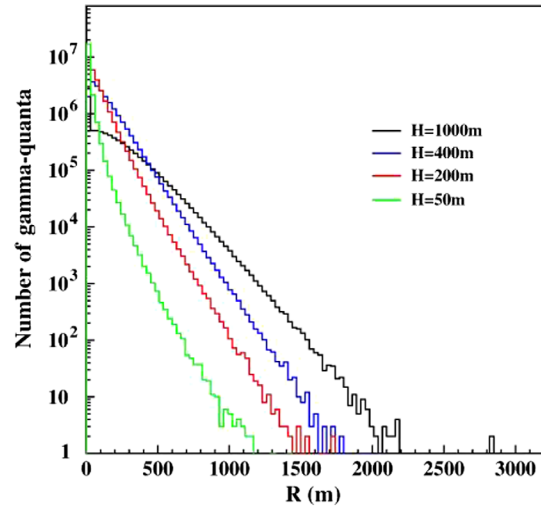


FIG. 14. Lateral distributions of gamma rays leaving thundercloud on different heights above the surface (located at 3200 m above sea level).

above Earth's surface. The particles were followed until $H_{\text{obs}} = 3200$ m above sea level. The secondary particle energy cut was $E = 0.05$ MeV; the lowest energy threshold of particle detectors operated on Aragats was 0.3 MeV. The cloud was located at four different heights: $H = 50$ m, 200 m, 400 m, and 1000 m above the observation level. In Fig. 14, we show the lateral distribution of gamma rays with energies above 0.3 MeV born in the cascade initiated by gamma rays leaving the thundercloud at different heights above the particle detectors.

In Fig. 14, we can see that scattered gamma rays from RRE avalanches can barely contribute to particle flux on distances larger than 1 km. Furthermore, as we see in Fig. 15, the zenith angle distribution for such gamma rays peaked on very large angles, making registration of gamma

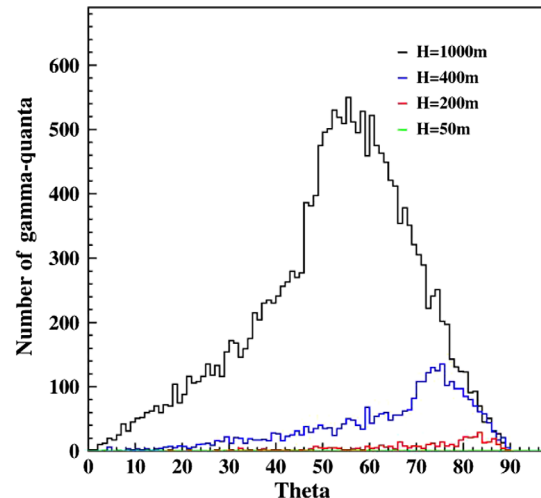


FIG. 15. Angular distributions of secondary gamma-quanta at distances $R > 1000$ m from the shower core.

rays with stacked horizontal particle detectors very problematic.

VI. VALIDATION OF MC SIMULATIONS

After verification of the simulation results performed by using different MC programs with the same parameters (we use CORSIKA and GEANT4 codes), the most important issue is the model validation, i.e., checking if the models used do more or less precisely describe the nature. The MC simulations described in the previous section were validated with a TGE that occurred on May 30, 2018, one of the four largest TGEs observed on Aragats in the last decade; see Fig. 16.

On May 30, the outside temperature was 1.61°C , dew point -0.86°C ; thus, the estimated height of the cloud base was $\approx 25\text{ m}$. Very high humidity of 98% also confirms very low location of the cloud base. The huge single peak (peak value of particle flux 76,000 per m, per m^2 , significance $\approx 78\% / 126\sigma$) shown in Fig. 16 occurred during the time span when the field was mostly in the negative domain ($\approx 25\text{ m}$, from 1:15 to 1:40). However, during the 4 minutes coinciding with the particle outburst, the near-surface electric field abruptly increased and remained in the positive domain. In analogy with Fig. 5, where we show the May 22 TGE, we can assume that, during this 4 minutes, a very strong LPCR was just above the detector site, producing a large electric field in the lower dipole of the cloud. Thus, the strength of the electric field in the lower dipole for a few minutes exceeded the runaway threshold

and, due to the low location of the cloud, a huge particle flux was registered.

The differential energy spectra of the May 30 TGE is posted in Fig. 17. Here, again, similar to the May 22 event (Fig. 6), we observe 3 minutes of HEP flux extrapolated with “broken” power law dependence. The power index for the low-energy (below 7–8 MeV) particle is very hard -1.2 , changing after turnover to a very steep one of ≈ -3 . And, again, before [Fig. 17(a)] and after [Fig. 17(c)] the minute of maximal flux [Fig. 17(b)], we observe the maximal energy of 20 MeV, at maximal flux -40 MeV . The difference between the May 22 and May 30 TGEs is the size of the LPCR deduced from the amplitude of the positive field excursion during the deep negative near-surface electric field. We can assume that because the distance of the cloud base is very small ($\approx 25\text{ m}$) on May 30, compared with May 22 ($\approx 100\text{ m}$), the influence of the LPCR on the total near-surface electric field is much larger. Thus, we have on May 30 one of the largest TGEs ever detected, with much larger intensity and significance than the May 22 TGE. We can explain the broken power law dependence as being due to a larger-than-usual LPCR that produced multiple avalanches that reached the ground and were registered. Thus, very large intensity of the TGE at energies below 8 MeV changed to an abrupt decline at higher energies (we already observed such a behavior; see Fig. 4 of [18]); the cumulative differential energy spectra measured by the MCAL calorimeter onboard the AGILE satellite also demonstrated very steep turnover at high energies [26]. After the decline of the TGE caused by the

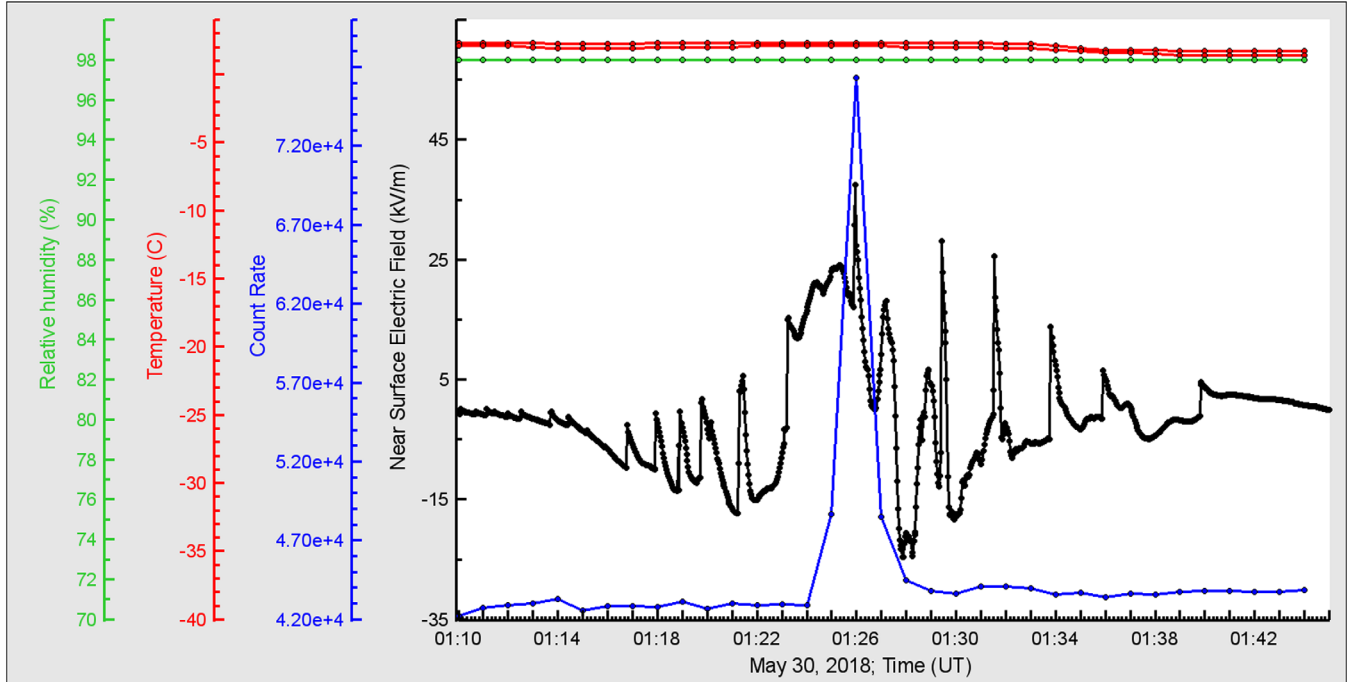


FIG. 16. Super-TGE occurred on May 30, 2018. At the top, outside temperature, dew point, and relative humidity and the middle disturbances of the near-surface electric field; at the bottom, 1-minute count rate of the 1-cm thick 1 m^2 -area outdoor plastic scintillator.

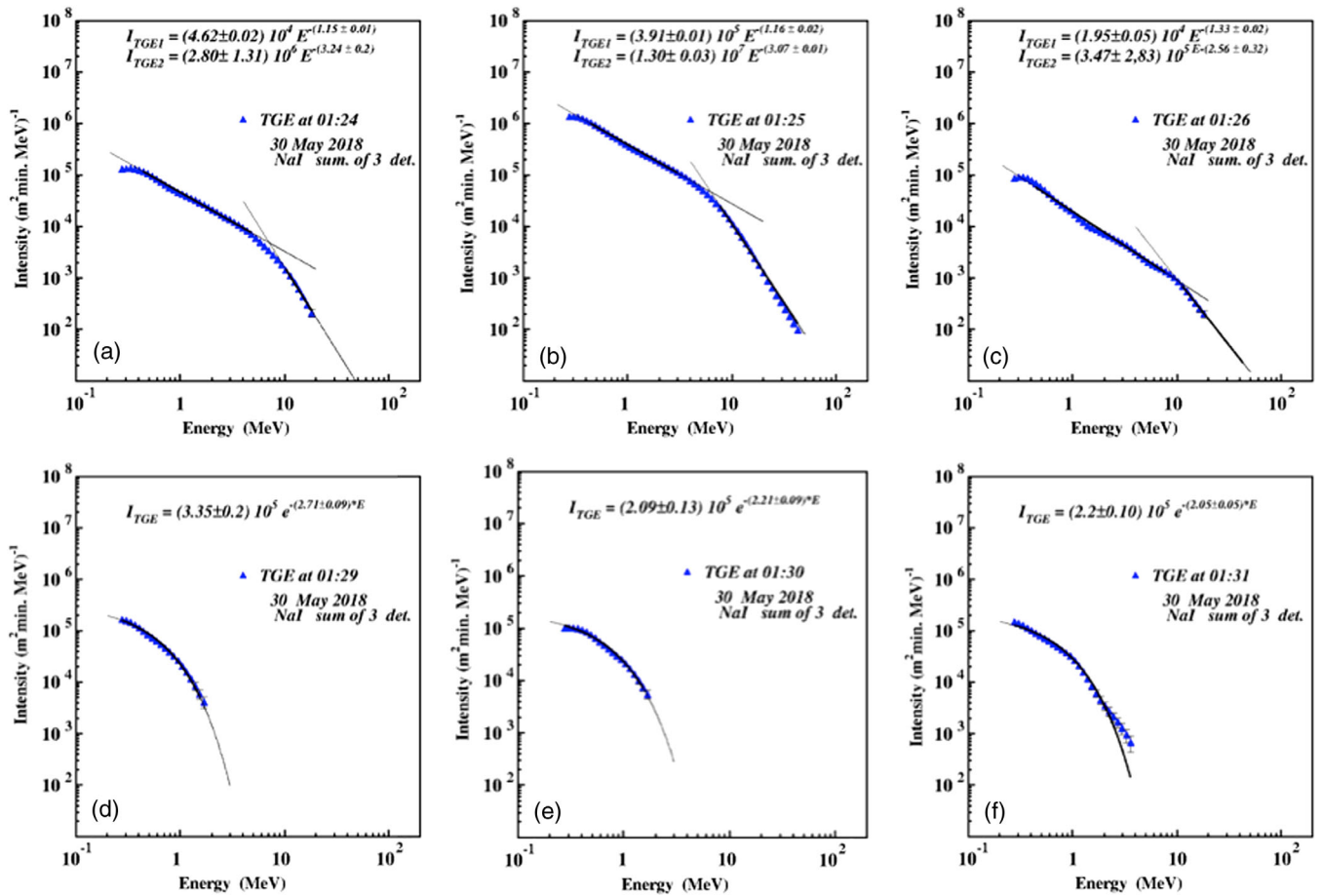


FIG. 17. The differential energy spectra of TGE particles registered by NaI network (N 1 and N 2 spectrometers); minutes 1:24–1:30.

near lightning flash, the particle flux continued for 1 hour with sizable count rate; however, the HEP particles disappeared [Figs. 6(d)–6(f)], the same as on May 22.

In Fig. 18, we show the differential energy spectra of the background gamma rays (obtained with WEB calculator PARMA/EXPACS, [27]), mostly originated from the interactions of the Galactic cosmic rays with the terrestrial atmosphere, and the spectrum measured by three large NaI crystals at 01:25 on May 30, 2018.

From the plots and from integral spectra shown in the left bottom corner, we see that overall TGE flux (mostly gamma rays with very small contamination of electrons) more than 2 times exceeds natural gamma radiation. Even after turnover (knee) at ≈ 8 MeV, TGE flux continues to exceed background until 20 MeV. Obtained integral spectra for 5 and 6 MeV thresholds well coincide with the fluxes observed by another particle detector—CUBE, supplied with veto effectively rejecting charged particles [28].

To gain insight into the size of the radiation-emitting region in the bottom of the cloud, we use measurements from the STAND1 particle detector network located on the

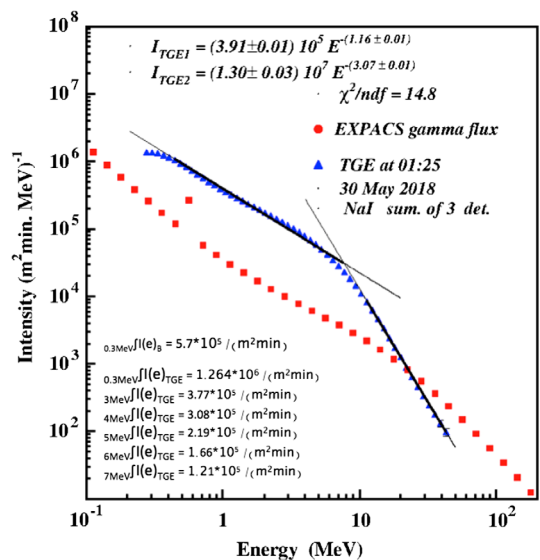


FIG. 18. Background spectrum and TGE spectrum observed on May 30, 2018. In the left bottom corner, values of integral spectrum calculated for different energy thresholds.

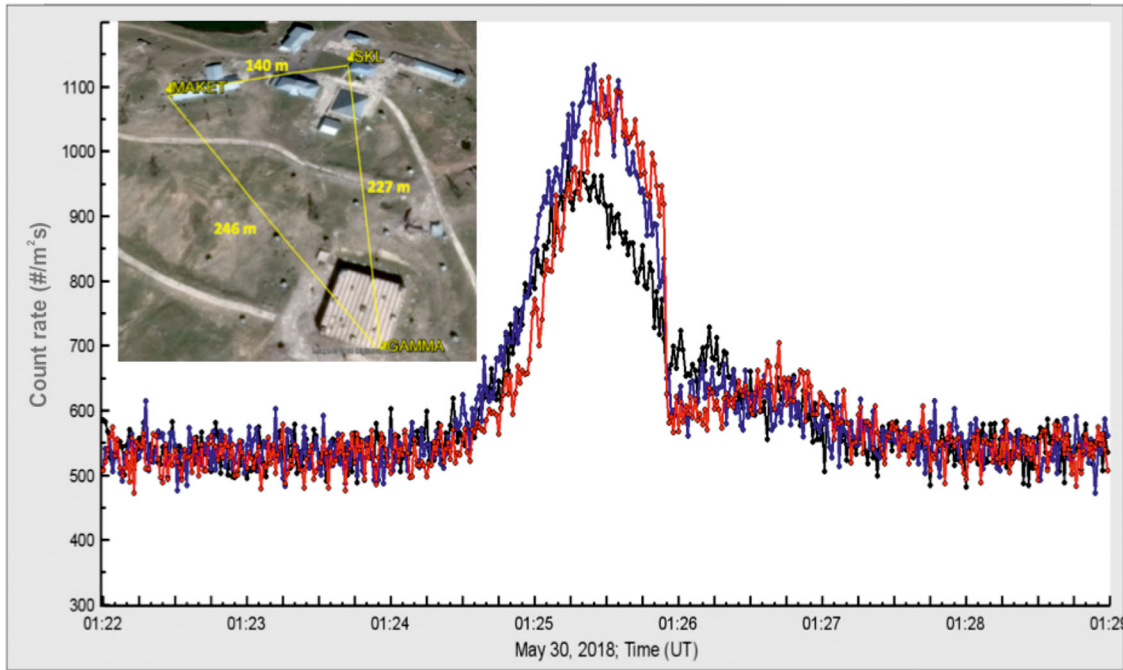


FIG. 19. One second time series of the STAND1 particle detector network count rates; in the inset, the map of detector units location.

Aragats station. In Fig. 19, we show the one-second time series of the May 30 TGE as measured by the three-cm-thick and one-m²-area outdoor plastic scintillators. The detectors are arranged in a triangle with unequal sides as shown in the inset in Fig. 19. Usually, the TGE measured by all three detectors coincides very well, as shown in the patterns of the one-second count rates displayed in Fig. 19; thus, the size of the emitting region in the cloud is rather large, exceeding at least 100 m.

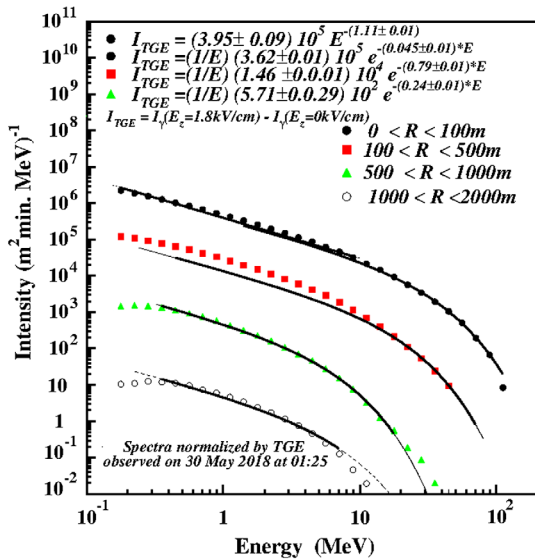


FIG. 20. Energy spectra of simulated TGE estimated by the particles fallen in the “rings” at different distances from the shower axes coincided with detector location site.

We use the recovered energy spectra at 1:25 on May 30 [Fig. 17(b)] for comparison and calibration of the simulated events containing high-energy particles. In Fig. 20, we present spectra of simulated events selected in different rings around the shower axes. We can see that, departing from the shower axes, the shape of the energy spectra become exponential and the maximal energy reduces in good agreement with observed energy spectra posted in Figs. 6, 9, and 17. We assume that when disturbances of the near-surface electric field calm down, but sizable flux of the TGE continues [see TGE intensities at 20:15–22:15, Fig. 4, and Figs. 6(d)–(f) and 17(d)–(f)], the electric field originated by the transient LPCR fades, and we can detect only low-energy gamma rays according to the MOS process and large-angle Compton scattered gamma rays.

The comparisons with simulation for such a complicated scientific domain as atmospheric electricity can provide only quantitative results. We are not aware of the localization and strength of intracloud electric fields. In simulations, we use the simplest tripole model with a uniform electric field between layers. The nature is much more complicated; nonetheless, TGEs give us new types of information (intensities and shapes of the “thundercloud” particle spectra) that overall agree with simulations.

VII. CONCLUSIONS

Observation of numerous TGEs by the Japanese, Chinese, and Slovakian groups [28–32] proves that RB/RREA and

MOS are robust and realistic mechanisms for electron acceleration and multiplication, confirming the correctness of the model of TGE initiation [5,13,33].

However, there are observations of the alternative source of thundercloud particles.

Physicists performing experiments at the Tien-Shan Mountain Cosmic Ray Station, Kazakhstan (altitude of 3340 m), reported the existence of high-energy emissions, i.e. the electron, gamma, and neutron fluxes that are directly from the lightning bolt [34]. Another observation of the lightning-induced gamma ray flux was reported by the group from the International Center for Lightning Research and Testing [35] in North Central Florida. The authors claimed the observation of very intensive gamma ray flux was associated with upward positive leaders approaching a negative charge region. The systematic research of the lightning-related x-ray radiation was made at the Lightning Observatory in Gainesville (LOG), Florida [36]. During a thunderstorm on February 6, 2017, in Japan, a γ -ray flash with duration of less than one millisecond was detected at monitoring sites 0.5–1.7 km away from the lightning. The subsequent γ -ray afterglow subsided quickly, with an exponential decay constant of 40–60 milliseconds, and was followed by prolonged line emission at about 0.511 MeV, which lasted for a minute [37]. Authors claimed conclusive evidence of positrons and neutrons being produced after the lightning. Few bursts of gamma ray showers have been observed coincident with downward-propagating negative leaders in lightning flashes by the Telescope Array Surface Detector [38]. The authors claimed that the observed energy deposit is consistent with forward-beamed showers of 10^{12} – 10^{14} or more primary photons above 100 keV, distributed according to a RREA spectrum. However, no model was presented to justify such a huge number of high-energy particles associated with a lightning flash.

During numerous storms observed from 2016 to 2018, we did not observe on Aragats any lightning producing relativistic particles in any of the continuously monitoring detectors. However, we do not exclude that propagation of lightning leaders and emerging of strong electric fields around leader tips can produce x rays and additional seed electrons involved in a runaway process. More registered events associated with lightning flash are needed to make a realistic model of such an exotic phenomenon.

In the present paper, we scrutinize the TGE model and propose the structure of the electric field in the thunderstorm atmosphere that accelerates and multiplies electrons, resulting in the huge particle fluxes reaching the Earth's surface.

The new key evidence, namely, intensities and energy spectra of the TGEs, along with associated disturbances of the near-surface electric field and lightning flashes, allows us to develop the comprehensive model of electric fields in the thundercloud. Discovered in 2017, long-lasting TGEs

prove that two independent mechanisms are responsible for bursts of high-energy particles and prolonged emissions of low-energy gamma rays.

HEP TGEs mostly occur when the near-surface electric field is in the deep negative domain and when the cloud base is 25–50 m above Earth's surface. The maximal energy of electrons in the RB/RREA avalanches can reach and exceed 40 MeV. Proof of the runaway process is the abrupt decline of the HEP bursts after the lightning flash, reestablished several seconds later when the electric field within the lower dipole again enhances the “runaway” threshold. Hours-long, low-energy gamma ray fluxes can be explained by the MOS process (modification of the cosmic ray electron energy spectra) in rather weak electric fields not triggering the RB/RREA process (low strength field originated between the main negative layer and its mirror on the Earth's surface).

LL TGEs start with small-intensity, low-energy gamma ray fluxes originated in weak electric fields between a mature main negative charge region in the middle of the cloud and its mirror on the Earth's surface. After several tens of minutes, or faster, with emerging of the LPCR above the detector site, the cumulative field surpasses the runaway threshold in the atmosphere, and the RB/REEA avalanches start in the cloud. If the cloud base is close to the Earth's surface (the case of Aragats storms in spring and autumn), TGE intensity can reach very high levels, exceeding the background radiation many times, and the maximal energy of the electrons and gamma rays reaches 40 MeV and more. Because the size of the LPCR is much smaller than the main negative region, the high-energy phase of the TGE is prolonged for only a few minutes, changing again to the low-energy gamma ray flux that can last for several hours.

The electron acceleration model based on the “classical” tripole charge structure of the thundercloud, which is used in our analysis [5,9,25], is the simplest one; however, we do not exclude more sophisticated scenarios of the electric field emergence in the thundercloud. Nearly (50%) of TGEs abruptly terminated by lightning flashes are associated not with cloud-to-ground but with normal-polarity intracloud flashes, signaling that charge of the main negative region is rather large and the lightning leader can make its path to the upper positively charged region. Another \approx 20% of TGEs abruptly terminated by lightning flashes are associated with inverted-polarity intracloud flashes. Observation of the TGE-terminating inverted-polarity IC flash which occurs in the lower dipole proves that the downward electron-accelerating electric field is significantly enhanced by the field formed by the main negative charge in the cloud and the LPCR and, thus, enables the TGE development. The inverted-polarity IC flash reduces the main negative charge and, thus, leads to the reduction or elimination of this field inside the cloud. As a result, the TGE is abruptly terminated.

Numerous TGEs observed on Aragats and appropriate Monte Carlo simulations confirm our model; however, many questions remain unanswered, including

- (i) The way of LPCR development;
- (ii) The size and shape of the particle-emitting region;
- (iii) The possible changes of radio emission patterns due to TGE propagation in the atmosphere [39];
- (iv) The influence of remote lightning flashes on disturbances of the near-surface electric field;
- (v) How the intracloud electric fields can be deduced from the ground-based measurements of the near-surface electric field.

In situ measurements of charge and field distribution in clouds by a Lightning Mapping Array (LMA) or interferometer

facilities (operation on Aragats begins in 2018) will improve our understanding of cloud electrification.

ACKNOWLEDGMENTS

The data for this paper are available via the multivariate visualization software ADEI on the web page of the Cosmic Ray Division (CRD) of the Yerevan Physics Institute, <http://adei.crd.yerphi.am/adei>. We thank the staff of the Aragats Space Environmental Center for the consistent operation of the Aragats research station facilities. We also thank E.Mareev and V.Rakov for useful discussions and appreciate the support of the Russian Science Foundation Grant (Project No. 17-12-01439).

-
- [1] J. R. Dwyer, The initiation of lightning by runaway air breakdown, *Geophys. Res. Lett.* **32**, L20808 (2005).
 - [2] E. R. Williams, The tripole structure of thunderstorms, *J. Geophys. Res.* **94**, 13151 (1989).
 - [3] X. Qie, T. Zhang, C. Chen, G. Zhang, T. Zhang, and X. Kong, Electrical characteristics of thunderstorms in plateau regions of China, *Atmos. Res.* **91**, 244 (2009).
 - [4] A. Nag and V. Rakov, Some inferences on the role of lower positive charge region in facilitating different types of lightning, *GRL* **36**, L05815 (2009).
 - [5] A. Chilingarian and H. Mkrtchyan, Role of the lower positive charge region (LPCR) in initiation of the thunderstorm ground enhancements (TGEs), *Phys. Rev. D* **86**, 072003 (2012).
 - [6] A. Chilingarian, A. Daryan, K. Arakelyan, A. Hovhannisan, B. Mailyan, L. Melkumyan, G. Hovsepyan, S. Chilingaryan, A. Reymers, and L. Vanyan, Ground-based observations of thunderstorm-correlated fluxes of high- energy electrons, gamma rays, and neutrons, *Phys. Rev. D* **82**, 043009 (2010).
 - [7] A. Chilingarian, G. Hovsepyan, and A. Hovhannisan, Particle bursts from thunderclouds: Natural particle accelerators above our heads, *Phys. Rev. D* **83**, 062001 (2011).
 - [8] A. Chilingarian, Y. Khanikyants, E. Mareev, D. Pokhsravian, V. A. Rakov, and S. Soghomonyan, Types of lightning discharges that abruptly terminate enhanced fluxes of energetic radiation and particles observed at ground level, *J. Geophys. Res. Atmos.* **122**, 7582 (2017).
 - [9] A. Chilingarian, G. Hovsepyan, and L. Vanyan, On the origin of the particle fluxes from the thunderclouds: Energy spectra analysis, *Europhys. Lett.* **106**, 59001 (2014).
 - [10] A. Chilingarian, B. Mailyan, and L. Vanyan, Observation of Thunderstorm Ground Enhancements with intense fluxes of high-energy electrons, *Astropart. Phys.* **48**, 1 (2013).
 - [11] A. Chilingarian, B. Mailyan, and L. Vanyan, Recovering of the energy spectra of electrons and gamma rays coming from the thunderclouds, *Atmos. Res.* **114–115**, 1 (2012).
 - [12] E. S. Cramer, B. G. Mailyan, S. Celestin, and J. R. Dwyer, A simulation study on the electric field spectral dependence of thunderstorm ground enhancements and gamma ray glows, *J. Geophys. Res. Atmos.* **122**, 4763 (2017).
 - [13] A. Chilingarian, Thunderstorm ground enhancements—Model and relation to lightning flashes, *J. Atmos. Terr. Phys.* **107**, 68 (2014).
 - [14] A. Chilingarian, G. Hovsepyan, Y. Khanikyanc, A. Reymers, and S. Soghomonyan, Lightning origination and thunderstorm ground enhancements terminated by the lightning flash, *Europhys. Lett.* **110**, 49001 (2015).
 - [15] A. V. Gurevich, G. M. Milikh, and R. A. Roussel-Dupre, Runaway electron mechanism of air breakdown and pre-conditioning during a thunderstorm., *Phys. Lett.* **165A**, 463 (1992).
 - [16] L. P. Babich, E. N. Donskoy, R. I. Il'kaev, I. M. Kutsyk, and R. A. Roussel-Dupre, Fundamental parameters of a relativistic runaway electron avalanche in air, *Plasma Phys. Rep.* **30**, 616 (2004).
 - [17] J. R. Dwyer, A fundamental limit on electric fields in air, *Geophys. Res. Lett.* **30**, 2055 (2003).
 - [18] A. Chilingarian, G. Hovsepyan, and L. Vanyan, On the origin of the particle fluxes from the thunderclouds: energy spectra analysis, *Europhys. Lett.* **106**, 59001 (2014).
 - [19] A. Chilingarian, G. Hovsepyan, and E. Mantasakanyan, Mount Aragats as a stable electron accelerator for atmospheric High-energy physics research, *Phys. Rev. D* **93**, 052006 (2016).
 - [20] T. C. Marshall, M. Stolzenburg, Paul R. Krehbiel *et al.*, Electrical evolution during the decay stage of New Mexico thunderstorms, *J. Geophys. Res.* **114**, D02209 (2009).
 - [21] A. Chilingarian, Long lasting low energy thunderstorm ground enhancements and possible Rn-222 daughter isotopes contamination, *Phys. Rev. D* **98**, 022007 (2018).
 - [22] A. Chilingarian, G. Hovsepyan, and B. Mailyan, In situ measurements of the runaway breakdown (RB) on Aragats mountain, *Nucl. Instrum. Methods Phys. Res., Sect. A* **874**, 19 (2017).

- [23] D. Heck, J. Knapp, J. N. Capdevielle, G. Schatz, and T. Thouw, Report No. FZKA 6019, 1998, Forschungszentrum, Karlsruhe, <https://www.ikp.kit.edu/corsika/70.php>.
- [24] S. Agostinelly, J. Allison, A. Amako *et al.*, Geant4—a simulation toolkit, *NIM* **506**, 250 (2003).
- [25] A. Chilingarian, S. Chilingaryan, T. Karapetyan, L. Kozliner, Y. Khanikyants, G. Hovsepyan, D. Pokhsrasyan, and S. Soghomonyan, On the initiation of lightning in thunderclouds, *Sci. Rep.* **7**, 1371 (2017).
- [26] M. Marisaldi, F. Fushino, M. Tavani *et al.*, Properties of terrestrial gamma ray flashes detected by AGILE MCAL below 30 MeV, *J. Geophys. Res. Space Phys.* **119**, 1337 (2014).
- [27] T. Sato, Analytical Model for Estimating the Zenith Angle Dependence of Terrestrial Cosmic Ray Fluxes, *PLoS One* **11**: e0160390 (2016).
- [28] T. Torii, T. Sugita, M. Kamogawa, Y. Watanabe, and K. Kusunoki, Migrating source of energetic radiation generated by thunderstorm activity, *Geophys. Res. Lett.* **38**, L24801 (2011).
- [29] H. Tsuchiya, T. Enoto, K. Iwata *et al.*, Hardening and Termination of Long-Duration Gamma Rays Detected Prior to Lightning, *Phys. Rev. Lett.* **111**, 015001 (2013).
- [30] Y. Kuroda, S. Oguri, Y. Kato, R. Nakata, Y. Inoue, C. Ito, and M. Minowa, Observation of gamma ray bursts at ground level under the thunderclouds, *Phys. Lett. B* **758**, 286 (2016).
- [31] B. Bartoli, P. Bernardini, X. J. Bi *et al.*, Observation of the thunderstorm-related ground cosmic ray flux variations by ARGO-YBJ, *Phys. Rev. D* **97**, 042001 (2018).
- [32] K. Kudela, J. Chum, M. Kollárik, R. Langer, I. Strhářský, and J. Baše, Correlations between secondary cosmic ray rates and strong electric fields at Lomnický štít, *J. Geophys. Res.* **122**, 10700 (2017).
- [33] A. Chilingarian, Long lasting low energy thunderstorm ground enhancements and possible Rn-222 daughter isotopes contamination, *Phys. Rev. D* **98**, 022007 (2018).
- [34] A. V. Gurevich, V. P. Antonova, A. P. Chubenko *et al.*, Strong Flux of Low-Energy Neutrons Produced by Thunderstorms, *Phys. Rev. Lett.* **108**, 125001 (2012).
- [35] B. M. Hare, M. A. Uman, J. R. Dwyer *et al.*, Ground-level observation of a terrestrial gamma ray flash initiated by a triggered lightning, *J. Geophys. Res. Atmos.* **121**, 6511 (2016).
- [36] S. Mallick, V. A. Rakov, and J. R. Dwyer, A study of X-ray emissions from thunderstorms with emphasis on subsequent strokes in natural lightning, *J. Geophys. Res.* **117**, D16107 (2012).
- [37] T. Enoto, Y. Wada, Y. Furuta *et al.*, Photonuclear reactions triggered by lightning discharge, *Nature (London)* **551**, 481 (2017).
- [38] R. U. Abassi, T. Aby-Zayyad, M. Allen *et al.*, Gamma-ray Showers Observed at Ground Level in Coincidence With Downward Lightning Leaders, *JGR Atmosphere* **123**, 6864 (2018).
- [39] P. Schellart, T. N. G. Trinh, S. Buitink *et al.*, Probing Atmospheric Electric Fields in Thunderstorms through Radio Emission from Cosmic-Ray-Induced Air Showers., *Phys. Rev. Lett.* **114**, 165001 (2015).